Applied Catalysis B: Environmental 91 (2009) 174–179

Contents lists available at ScienceDirect

Applied Catalysis B: Environmental

journal homepage: www.elsevier.com/locate/apcatb

The role of α-sites in N_2O decomposition over FeZSM-5. Comparison with the oxidation of benzene to phenol

L.V. Pirutko *, V.S. Chernyavsky, E.V. Starokon, A.A. Ivanov, A.S. Kharitonov, G.I. Panov **

Boreskov Institute of Catalysis, SB RAS, Pr. Akad. Lavrentieva, 630090 Novosibirsk, Russia

ARTICLE INFO

Article history:
Received 26 March 2009
Received in revised form 14 May 2009
Accepted 18 May 2009
Available online 23 May 2009

Keywords:
N_2O decomposition
N_2O reduction
FeZSM-5
α-Sites
α-Oxygen
Benzene oxidation

ABSTRACT

The kinetics and the mechanism of nitrous oxide decomposition (NOD) were studied using a set of FeZSM-5 samples with a wide variation in concentration of α-sites, which are special complexes of bivalent iron $(Fe^{II})_\alpha$ stabilized in the micropore space of the zeolite matrix. The results are compared with the N_2O oxidation of benzene to phenol (OBP) studied earlier with the same set of samples. In spite of strong differences in turnover frequencies (ca. 100 times) and activation energies (92 kJ/mol), both reactions are catalyzed by the same active centers represented by α-sites. The rates of the reactions increase linearly with increasing α-sites concentration within two orders of magnitude.

The NOD and OBP reactions are shown to have kindred mechanisms, which can be described by two main steps. The first step is a common one and includes oxidation of the α-site by the deposition of α-oxygen from N_2O:

$$(Fe^{II})_\alpha + N_2O \rightarrow (Fe^{III}{-}O^-)_\alpha + N_2$$

The α-oxygen can be safely quantified, its properties being thoroughly studied in many previous works.

The second step is the reduction of the site. It proceeds due to the removal of α-oxygen by the interaction of the latter with either N_2O (NOD reaction) or benzene (OBP reaction). In both cases this step is the rate determining one.

Mechanistically, the OBP can be considered as an N_2O reduction by benzene. One may think that fundamental role of α-sites may hold also for N_2O reduction by other substrates like CO, methane, propane, etc., which are widely used for this purpose.

1. Introduction

Due to the greenhouse and ozone-depleting effects industrial emissions of nitrous oxide raises an ever-growing ecological concern. For solving the problem two ways are considered to be most efficient [1–5]: N_2O decomposition to the constituting elements in the case of its diluted off-gases (e.g. nitric acid plants), and the use of N_2O as a selective oxygen donor in the case of its concentrated off-gases (e.g. adipic acid plants). The reaction of N_2O reduction is also considered to be a promising if cheap reducing agents are available on on-site.

Of numerous samples tested in the direct nitrous oxide decomposition (NOD):

$$N_2O \rightarrow N_2 + (1/2)O_2 \quad (1)$$

Fe-containing ZSM-5 zeolites are among the most active catalysts [1–3]. In distinction to other catalysts, O_2 admixture exhibits no deactivation effect on FeZSM-5, while NO admixture even increases the reaction rate. This makes FeZSM-5 zeolites a unique system capable of stable operation with realistic off-gases containing O_2, NO and H_2O. Uhde Ltd. used FeZSM-5 to develop the EnviNO_x process for simultaneous abatement of N_2O and NO in the off-gases of nitric acid plants [3].

The most known example of the second way is an N_2O use for the oxidation of benzene to phenol [4,5]:

$$C_6H_6 + N_2O \rightarrow C_6H_5OH + N_2 \quad (2)$$

A new pilot scale process has been developed on this basis providing a nearly 100% selectivity for phenol. Surprisingly, FeZSM-5 zeolites happened to be the best catalysts for this reaction, too. It gives an idea that, in addition to a common N_2O reagent, reactions (1) and (2) may have a more deep relationship arising from their mechanistic similarity.

Many works were devoted to the mechanism of these reactions, of which the oxidation of benzene to phenol (OBP) was studied

* Corresponding author. Tel.: +7 383 326 97 93.
** Corresponding author. Tel.: +7 383 330 94 52.
E-mail addresses: pirutko@catalysis.ru (L.V. Pirutko), panov@catalysis.ru (G.I. Panov).

0926-3373/$ – see front matter © 2009 Elsevier B.V. All rights reserved.
doi:10.1016/j.apcatb.2009.05.021

most thoroughly. Special extra-lattice complexes of bivalent iron stabilized in the micropore space of FeZSM-5 matrix (called α-sites) were shown to be active sites of this reaction. A remarkable feature of these sites is that, being inert towards dioxygen, they readily react with nitrous oxide to generate anion radical oxygen species (called α-oxygen) [4–12]:

$$N_2O + (Fe^{II})_\alpha \rightarrow (Fe^{III}{-}O^-)_\alpha + N_2 \quad (3)$$

α-Oxygen was shown to be the active species that performs the oxidation of benzene to phenol [13,14]. It has a low binding energy to the surface and a very high reactivity, which shows itself at room and even lower temperatures towards various substrates including methane [4]. This high reactivity strongly differentiates O_α from the rest surface oxygen and provides a nice opportunity for measuring both the α-oxygen amount and the α-site concentration. Such a measurement is usually made in a static vacuum unit using some low-temperature test reactions, of which the $^{18}O_2/^{16}O_\alpha$ isotopic exchange is the most convenient one [15,16]. A flow unit can be also used for the purpose [17–21], although for the reasons discussed elsewhere [16] the accuracy in this case may be not so high.

The mechanism of NOD reaction is less clear. Unlike the OBP, for which most authors use the FeZSM-5 zeolites of similar preparation and composition, here a broad variety of FeZSM-5 samples are used. They strongly differ in the iron content, methods of its introduction (at the step of zeolite synthesis, by impregnation, by liquid-phase ion exchange, solid-phase ion exchange, CVD [18–28]), and activation conditions [8,23,27–32]. This leads to a variety of Fe states that form both in the micropore space and at the external surface of the zeolite matrix, and are observed by many spectroscopic techniques (XRD, EPR, NMR, IR, Mössbauer, EXAFS, RIXS, etc.). But these techniques do not allow a reliable quantification of the states. Therefore one fails to make a quantitative comparison of the results with the reaction rate, which would be the most convincing way for identifying the catalytically active Fe species.

In this connection, one may note a rather surprising circumstance related to α-sites. Although these sites can be easily quantified, their role in the NOD reaction was poorly investigated. In some papers [18–20] the reaction rate was compared with C_α values and almost linear correlations were obtained. However, the authors paid little attention to this result, focusing mainly on other aspects of the works. A linear correlation between r_{N_2O} and C_α was observed also in [33] where the NOD was studied with a vacuum unit.

In the present work, we perform a systematic study on the role of α-sites in the NOD reaction. The work is carried out with the same set of FeZSM-5 samples that has been studied earlier in the OBP reaction [14]. As we will see further, a comparison of the data obtained with these two reactions identifies their kindred mechanisms due to a key role of α-sites in both cases.

Note that a similar comparative study was made earlier by Zhu et al. [34]. The authors found that both NOD and OBP reactions proceed on analogous FeZSM-5 sites. However, later they changed their mind [20], concluding that NOD reaction is catalyzed by oligonuclear iron species while the OBP is catalyzed by mononuclear species.

2. Experimental

2.1. Samples

FeZSM-5 samples (Table 1) were prepared by hydrothermal synthesis using alumosilicate (AS), borosilicate (BS) and titanium-silicate (TS) zeolite matrices, and denoted according to the earlier accepted nomenclature [13,14]. For example, AS(0.18 Fe) corresponds to the zeolite of alumosilicate composition with iron content 0.18 wt.%, and BS(1.0 Fe) corresponds to the zeolite of borosilicate composition with iron content 1.0 wt.%. The initial zeolite matrices (without Fe) had the following atomic ratios of silicon to heteroatom: Si/Al = 56; Si/B = 72; Si/Ti = 32. Prior to catalytic testing, the samples were steam activated at 650 °C in a helium flow containing 50 mol.% H_2O. The XRD analysis showed that all samples have the MFI structure and a high crystallinity.

The concentration of α-sites (Table 1) was measured in a static vacuum unit, based on an amount of N_2 evolved by reaction (1) and on the isotopic $^{16}O_\alpha/^{18}O_2$ exchange. More information on the samples is given elsewhere [13,14].

2.2. Catalytic properties

Catalytic properties in NOD reaction were tested in an automated flow unit with chromatographic analysis of the gas phase. Generally, 1 g of catalyst (ca. 2 cm^3, fraction 0.5–1.0 mm) was loaded in a quartz reactor of 7 mm i.d. The feed mixture comprised 5.5 mol.% N_2O in a He flow. This N_2O concentration was chosen for the reason of a more safe comparison with the OBP data obtained earlier with the feed mixture comprising also 5.5 mol.% N_2O [14]. The feed rate was 2 cm^3/s and W/F = 0.5 g s/cm^3. Before testing, the catalyst was pretreated in the reaction mixture at 823 K for 2 h, cooled to 723 K, and purged with He for 20 min.

The decomposition of nitrous oxide was typically conducted at a temperature-programmed heating with 1 K/min ramp in the range of 573–873 K. The reaction mixture was sampled periodically for a TCD chromatographic analysis using a packed column filled with Porapak Q. A rate constant referred to catalyst weight

Table 1
N_2O decomposition over Fe-ZSM-5 catalysts.

Catalyst (wt.% Fe)	$C_\alpha \times 10^{-17}$, site/g	Rate constants at 698 K				Reaction rates at 648 K, mmol N_2O/g h	
		$k_w \times 10^2$, mmol N_2O/g s	k_{Fe}, mmol N_2O/mmol Fe s	k_α, mmol N_2O/mmol site s	E, kJ/mole	r_{N_2O} [a]	$r_{N_2O+C_6H_6}$ [b]
AS(0.006 Fe)	0.6	0.009	0.084	0.9	235	0.0016	0.5
AS(0.03 Fe)	6.5	0.22	0.41	2.0	201	0.018	2.9
AS(0.05 Fe)	20	0.63	0.71	1.9	218	0.054	6.8
AS(0.18 Fe)	60	2.20	0.68	2.2	214	0.16	19
AS(0.53 Fe)	190	5.80	0.60	1.8	209	0.51	53
BS(0.24 Fe)	1.3	0.07	0.016	3.0	218	0.0035	2.3
BS(1.00 Fe)	30	1.10	0.06	2.2	205	0.08	10
TS(0.95 Fe)	55	2.60	0.15	2.8	209	0.15	19
TS(1.8 Fe)	92	4.20	0.13	2.7	201	0.25	29

[a] 5.5 mol.% N_2O, balance He, W/F = 0.5 g s/cm^3.
[b] 5.5 mol.% N_2O, 50 mol.% C_6H_6, balance He, W/F = 0.5 g s/cm^3.

was calculated by Eq. (4), commonly used for this first order catalytic reaction [19,20,32]:

$$k_w = \frac{\ln(1-X)\cdot F}{W\cdot P} \quad (4)$$

where X is an N_2O conversion, F is a feed flow, W is a catalyst weight, and P is a total pressure equal to 1 atm. Accordingly, the rate of N_2O decomposition was calculated by Eq. (5):

$$r_{N_2O} = k_w P_{N_2O} \quad (5)$$

where P_{N_2O} is a partial pressure of N_2O. At low N_2O conversions, r_{N_2O} can be obtained directly from the concentrations of reaction products.

To calculate a rate constant referred to a Fe atom (k_{Fe}) or to an α-site (k_α), a k_w value was divided by the concentration of Fe or by the concentration of α-sites, respectively.

3. Results

3.1. Preliminary experiments

To obtain correct catalytic results at a TP-heating, one should be certain that at each temperature the catalyst is operating under thermal equilibrium and the reaction proceeds in a quasistationary mode. The feasibility of this condition needs a special verification in each case. In our experiments, to decrease a catalyst overheating by the reaction heat (81.6 kJ/mol), we used a weighty sample, bed depth of which in the reactor was over 50 mm. We also performed some preliminary runs to verify our experimental procedure. The runs were conducted with AS(0.05 Fe) sample having a representative catalytic activity.

Fig. 1 shows N_2O conversion as a function of temperature. Runs 1 and 2 are sequential experiments carried out at different ramps, 1 K/min and 2 K/min. Run 3 was performed after run 2 at a stepwise cooling to ensure safe isothermal condition of the reaction. In this case, the temperature was programmed to decrease stepwise from 773 to 623 K at a 5 K ramp. At each reaction temperature, the catalyst was kept for 30 min before registration of the N_2O conversion. Run 4 was performed at a standard TP-heating of 1 K/min with a lower concentration of nitrous oxide (1.0 mol.%).

As seen from Fig. 1, results of all these runs within experimental error (5 rel.%) fall on a common profile. Therefore we may conclude that no noticeable overheating of the catalyst takes place with our procedure, and the reaction proceeds in a quasistationary mode. The coincidence of conversions at 5.5 mol.% and 1.0 mol.% N_2O indicates the first reaction order, which agrees with the literature data [35–38]. The mole ratio N_2:O_2 in the reaction products was 2:1.

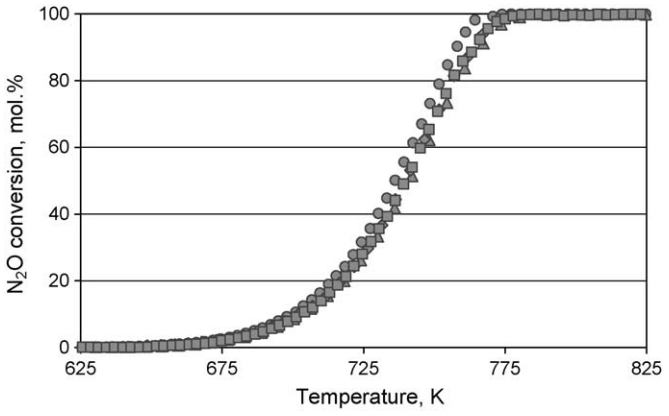

Fig. 1. N_2O conversion vs. temperature over AS(0.05 Fe) at different experimental conditions: (1) heating 1 K/min, 5.5 mol.% N_2O (circle); (2) heating 2 K/min, 5.5 mol.% N_2O (triangle); (3) stepwise cooling, 5.5 mol.% N_2O (rhomb); (4) heating at 1 K/min, 1.0 mol.% N_2O (square).

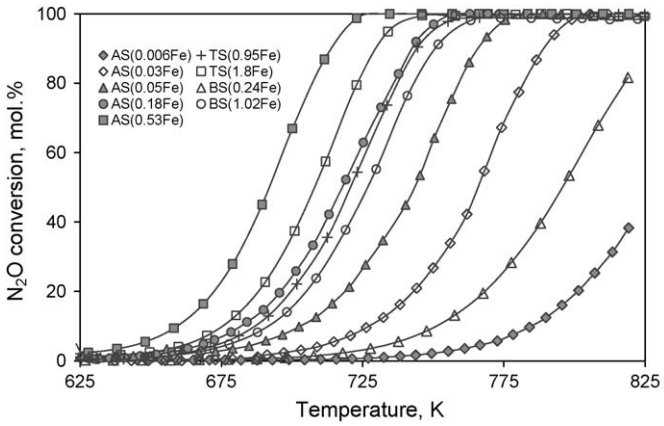

Fig. 2. N_2O conversion vs. temperature over FeZSM-5 zeolites (5.5 mol.% N_2O, 1 K/min).

3.2. Temperature dependence

The results of N_2O decomposition for all samples studied are shown in Fig. 2.

There is a strong variation of catalytic activity. Thus, at 723 K the conversion of N_2O over AS(0.006 Fe) is 2.5%, whereas over AS(0.53 Fe) it is 100%. Table 1 presents rate constants k_w at 698 K, which values for different samples differ by more than two orders of magnitude.

Fig. 3 shows Arrhenius plots of k_w constants. Even at first sight one may notice that, in spite of a considerable shift over the ordinate, all the plots have a close slope, which indicates close activation energies. Indeed, E values calculated from these data differ only slightly and fall within a range of 200–235 kJ/mol (Table 1).

3.3. The role of α-sites

As a first approximation one may think that different catalytic activity of FeZSM-5 samples results from different iron content. Indeed, with a growing Fe content in alumosilicate samples (Table 1), k_w value at 698 K increases from 9×10^{-5} mmol/g s for AS(0.006 Fe) to 5.8×10^{-2} mmol/g s for AS(0.53 Fe). However, the increase is not proportional. This is especially clearly seen when

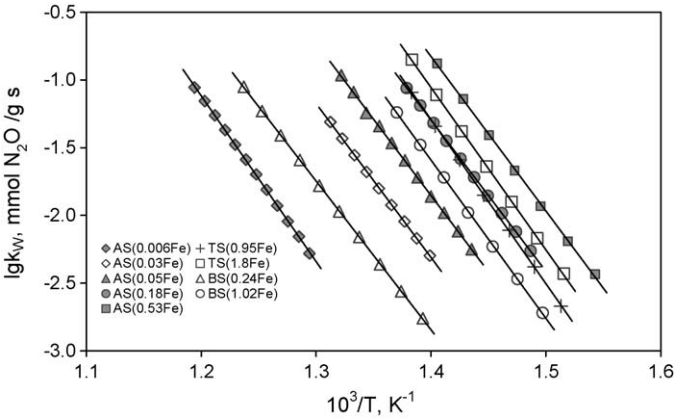

Fig. 3. Arrhenius plots for N_2O decomposition over FeZSM-5 zeolites.

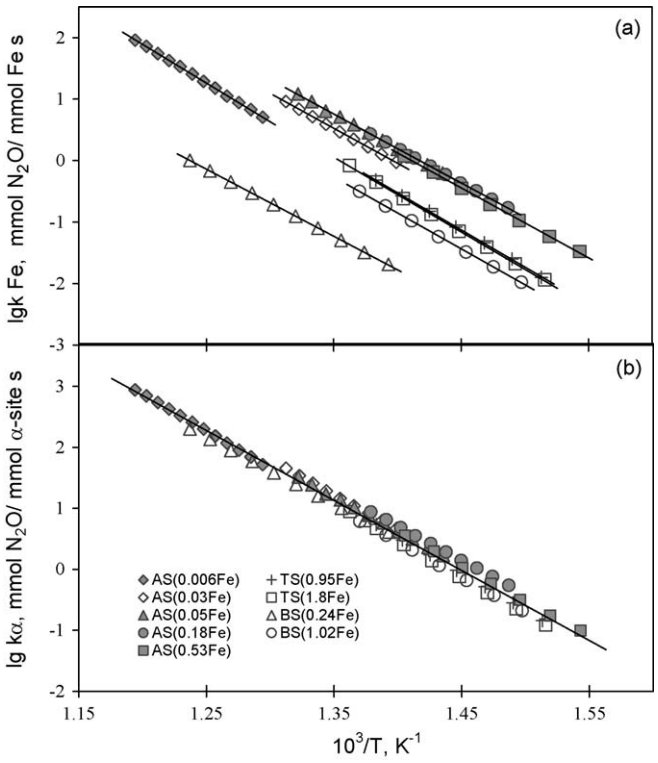

Fig. 4. Arrhenius plots of rate constants k_{Fe} (a) and k_{α} (b).

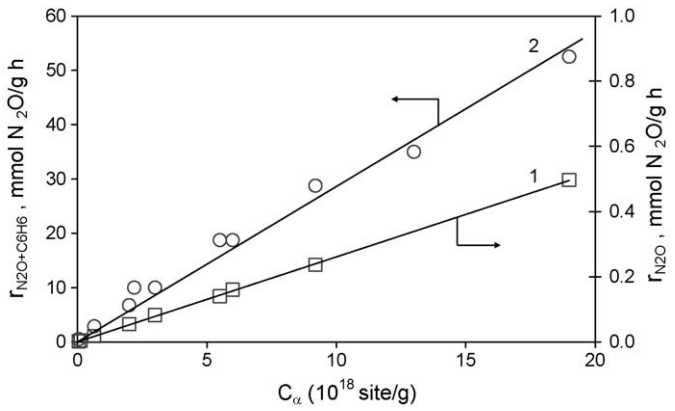

Fig. 5. Rates of N_2O decomposition (1) and benzene oxidation to phenol (2) at 648 K vs. α-site concentration (with the data of Table 1).

going to the samples of borosilicate and titaniumsilicate composition. In the latter cases, k_w values happen to be small as compared to the Fe contents. This indicates that only a part of iron, variable from sample to sample, is catalytically active. Indeed, the atomic rate constant k_{Fe} referred to the total iron content varies for the studied samples by more than an order of magnitude, from 0.016 mmol N_2O/mmol Fe s in the case of BS(0.24 Fe) to 0.71 mmol N_2O/mmol Fe s in the case of AS(0.05 Fe).

Now let's consider the data in the light of α-sites activity. Indeed, one may assume that, similar to the oxidation of benzene to phenol, the active part of Fe for the NOD reaction is also represented by α-sites. If so, the rate constant k_{α} referred to the concentration of α-sites should have close values in all cases. Table 1 confirms well this expectation. The variation of k_{α} is not significant, and its average value equals 2.4 ± 0.6 mmol N_2O/mmol α-site s. A somewhat lower k_{α} for AS(0.006 Fe) may relate to insufficient accuracy of a very low concentration of α-sites in this case.

Theoretically, this remarkable constancy of k_{α} may happen just to be an accidental result valid only at the chosen comparison temperature, 698 K. However, Arrhenius plots presented in Fig. 4 disagree with this idea. In distinction to quite scattered dependences for k_w (Fig. 3), the dependences for k_{Fe} are much closer (Fig. 4a), and those for the k_{α} practically merge into a single line (Fig. 4b), which satisfactorily describes experimental data over the entire range of temperatures. A slope of this line corresponds to the activation energy $E = 218 \pm 16$ kJ/mol.

A constant value of k_{α} leads to an excellent linear dependence of the NOD reaction rate on the concentration of α-sites plotted with the data of Table 1 (Fig. 5, line 1). In this connection, it is reasonable to mention some previous works on N_2O decomposition over Fe-containing zeolites [18–21]. Using various flow procedures (N_2O reoxidation after Fe autoreduction [19], O_{α} desorption [18], CH_4 reactivity test [20], H_2-TPD [21]) some authors performed quantification of the oxygen deposited from N_2O (but not O_2). Although different authors called this oxygen differently, there is a little doubt that in all cases the same type of oxygen was discussed, which we call the α-oxygen. All the above-mentioned authors revealed rather fair linear dependences of the NOD activity on the amount of this N_2O-derived oxygen, similar to the dependence in Fig. 5.

4. Discussion

4.1. Mechanism of nitrous oxide decomposition

The kinetics and the mechanism of nitrous oxide decomposition were studied in many works using different type catalysts including metals, metal oxides and zeolites. Results of these studies were considered in several reviews [1–4,39,40]. Two main hypotheses on the reaction mechanism are discussed. The first mechanism was suggested in early NOD studies made over oxide catalysts [39]. This mechanism is described by a classic scheme, which simplified form consists of two steps: N_2O dissociation resulting in the oxygen adsorbed on the surface; and O_2 desorption via recombination of the surface oxygen. In our case, with the involvement of α-sites, this mechanism can be presented as follows:

Mechanism I

$$N_2O + (Fe^{II})_{\alpha} \rightarrow (Fe^{III}{-}O^{-})_{\alpha} + N_2 \quad \text{(I-1)}$$

$$2(Fe^{III}{-}O^{-})_{\alpha} \rightarrow 2(Fe^{II})_{\alpha} + O_2 \quad \text{(I-2)}$$

The second mechanism was proposed by Fu et al. [35] to explain some kinetic features observed with Fe-Y and Fe-MOR zeolites, viz, the first order with respect to N_2O and the lack of inhibition by O_2. An original and rather surprising idea of the authors was that nitrous oxide in its reaction with active sites can serve as both an oxidizing and reducing agent. This mechanism can also be presented by two main steps:

Mechanism II

$$N_2O + (Fe^{II})_{\alpha} \rightarrow (Fe^{III}{-}O^{-})_{\alpha} + N_2 \quad \text{(II-1)}$$

$$N_2O + (Fe^{III}{-}O^{-})_{\alpha} \rightarrow (Fe^{II})_{\alpha} + N_2 + O_2 \quad \text{(II-2)}$$

Step (II-1) is identical to step (I-1). Here N_2O oxidizes the α-site by depositing the α-oxygen. At step (II-2), another molecule of N_2O interacts with the oxidized site to evolve O_2 and to reduce the site. Actually, step (II-2) may have a more complicated mechanism consisting of several elementary stages. Based on theoretical calculations, kinetic and TAP experiments, some authors [37,41–

44] suggested detail descriptions of this step. In particular, it may include intermediate formation of bi-atomic oxygen species on the active site, followed by its transformation into adsorbed O_2 molecule, which finally desorbs into the gas phase.

In the case of zeolites, neither of these mechanisms still received a conclusive experimental evidence. Some authors interpret their results in favor of the mechanism I [8,19,20,29,41] and the others in favor of the mechanism II [23,42–44]. However, all the researchers agree that the first step of both mechanisms (the N_2O dissociation) is fast and does not limit the reaction rate. Indeed, with α-sites this step proceeds at 473–523 K and has as low activation energy as 42 kJ/mol [15]. For comparison, Wood et al. [37] reported activation energy of 70 kJ/mol for this step. Extrapolation of these results to the reaction conditions used in the present work shows that the N_2O dissociation with α-oxygen loading at 698 K should be 100–200 times faster than the observed NOD rate. Therefore, main mechanistic problem is a second reaction step related to the oxygen removal. The following alternative should be solved: whether the removal proceeds by O_α recombination (Eq. (I-2)) or by the reaction with N_2O (Eq. (II-2)).

A linear dependence presented in Fig. 5 provides a new important argument for solving this problem. The dependence clearly identifies the first kinetic order of the reaction with respect to α-sites, $n_\alpha = 1$. This order is consistent with the step (II-2), but is not consistent with the recombination step (I-2), since the latter one needs $n_\alpha = 2$.

4.2. Comparison of NOD and OBP reactions

These two reactions consider nitrous oxide from the opposite points of view. For NOD reaction, N_2O is an ecologically unfriendly substance that should be destroyed. For the OBP, on the contrary, N_2O is a valuable oxygen donor that affords very high selectivity for phenol, which is impossible with other oxidants [4,5]. Nevertheless here, for the comparison purpose, we will consider the OBP from ecological point of view, i.e. as an N_2O reduction by benzene, similar to its reduction by CO, methane, ethane and other hydrocarbons [27,45–49].

In this connection, of numerous works devoted to the OBP, most interesting is the work by Chernyavsky et al. [14], conducted with the same FeZSM-5 samples as those used in our present work. To exclude extrapolation and obtain the most reliable dependence on the concentration of α-sites, the reaction rate in [14] over all samples was measured at the same temperature, 648 K. For that, depending on the C_α value, the weight of a sample was varied from 0.04 g to 1.05 g so as to load an equal amount of α-sites in the reactor. The results on the OBP reaction published in [14] are used further for comparison with the NOD data.

Fig. 5 shows the rate of N_2O decomposition (1) and that of benzene oxidation by N_2O (2) at 648 K versus α-sites concentrations. Both rates are expressed in the same units, mmol N_2O/g h. One can see that the rate of OBP is much higher than that of the NOD indicating that benzene strongly accelerates the process. Thus, at $C_\alpha = 10 \times 10^{18}$ α-site/g, without benzene $r_{N_2O} = 0.27$ mmol N_2O/g h, whereas with benzene $r_{N_2O+C_6H_6} = 28$ mmol N_2O/g h, which corresponds to a 100-fold difference in the reaction turnover frequency calculated per α-site. A scale of this difference may vary with changing reaction conditions, but in any case the step of α-oxygen removal by benzene:

$$C_6H_6 + (Fe^{III}{-}O^-)_\alpha \rightarrow C_6H_5OH + (Fe^{II})_\alpha \quad (5)$$

is obviously much more efficient than that by N_2O (Eq. (II-2)). The activation energy of OBP reaction is 126 kJ/mol [50], which is by 92 kJ/mol lower than in the case of NOD. Such a strong acceleration effect is typical of all reducing reagents [29,45–49]. Therefore, one may think that, similar to the reduction by benzene, α-sites may also play a fundamental role in other processes of N_2O reduction important for its abatement in off-gases.

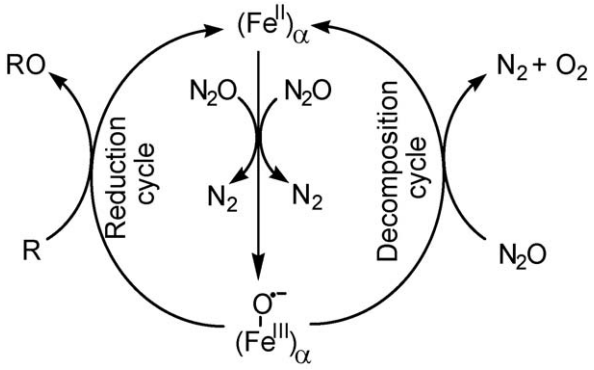

Fig. 6. Catalytic cycles of N_2O decomposition and N_2O reduction on α-sites.

Fig. 6 presents a general mechanistic scheme summarizing our results. According to this scheme both reactions proceed via reversible redox transition $Fe_\alpha^{II} \leftrightarrow Fe_\alpha^{III}$ that takes place in the presence of N_2O. The initial bivalent iron is oxidized by N_2O due to a loading of α-oxygen. Further, depending on process conditions, the oxidized site may alternatively react either with another N_2O molecule (decomposition cycle) or with a reductant molecule (reduction cycle). Both routes restore the initial state of α-site.

5. Conclusions

The catalytic decomposition of N_2O over FeZSM-5 zeolites is shown to be provided by α-sites, which concentration varies within two orders of magnitude and determines directly the rate of the reaction. The results are compared with the data on oxidation of benzene to phenol with N_2O. The latter reaction has been studied earlier with the same set of samples and shown to be catalyzed also by α-sites. The identity of active centers gives rise to kindred mechanisms of the reactions. In both cases the rate limiting step relates to α-oxygen removal from the oxidized α-site. In the case of NOD reaction α-oxygen is removed by interaction with N_2O, whereas in the case of OBP reaction by interaction with benzene. The removal by benzene is highly efficient compared to N_2O. Therefore the latter reaction has a much lower activation energy (126 kJ/mol against 218 kJ/mol) and a much higher turnover frequency, exceeding that of NOD by ca. 100 times.

α-Sites may also be of key importance for N_2O reduction by various reducing components.

Acknowledgement

The authors acknowledge financial support by the Russian Foundation for Basic Research (project 06-03-72551).

References

[1] F. Kapteijn, J. Rodriguez-Mirasol, J.A. Moulijn, Appl. Catal. B: Environ. 9 (1996) 25–64.
[2] G. Centi, S. Perathoner, F. Vazzana, M. Marella, M. Tomaselli, M. Mantegazza, Adv. Environ. Res. 4 (2000) 325–338.
[3] J. Perez-Ramirez, F. Kapteijn, K. Schoffel, J. Moulijn, Appl. Catal. B: Environ. 44 (2003) 117–151.
[4] G.I. Panov, CATTECH 4 (2000) 18–28.
[5] V.N. Parmon, G.I. Panov, A.K. Uriarte, A.S. Noskov, Catal. Today 100 (2005) 115–131.
[6] K.A. Dubkov, N.S. Ovanesyan, A.A. Shteinman, E.V. Starokon, G.I. Panov, J. Catal. 207 (2002) 341–352.
[7] S. Malykhin, I. Zilberberg, G.M. Zhidomirov, Chem. Phys. Lett. 414 (2005) 434–437.
[8] P.K. Roy, G.D. Pirngruber, J. Catal. 227 (2004) 164–174.

[9] J. Taboada, A. Overweg, P.J. Kooyman, I.W.C.E. Arends, G. Mul, J. Catal. 231 (2005) 56–66.
[10] G.I. Panov, K.A. Dubkov, E.V. Starokon, Catal. Today 117 (2006) 148–155.
[11] G.D. Pirngruber, J.-D. Grunwaldt, P.K. Roy, J.A. van Bokhoven, O. Safonova, P. Glatzel, Catal. Today 126 (2007) 127–134.
[12] E. Berrier, O. Ovsitser, E.V. Kondratenko, M. Schwidder, W. Grünert, A. Brückner, J. Catal. 249 (2007) 67–78.
[13] L.V. Pirutko, V.S. Chernyavsky, A.K. Uriarte, G.I. Panov, Appl. Catal. A: Gen. 227 (2002) 143–157.
[14] V.S. Chernyavsky, L.V. Pirutko, A.K. Uriarte, A.S. Kharitonov, G.I. Panov, J. Catal. 245 (2007) 466–469.
[15] G.I. Panov, A.K. Uriarte, M.A. Rodkin, V.I. Sobolev, Catal. Today 41 (1998) 365–385.
[16] G.I. Panov, E.V. Starokon, L.V. Pirutko, E.A. Paukshtis, V.N. Parmon, J. Catal. 254 (2008) 110–120.
[17] L. Kiwi-Minsker, D.A. Bulushev, A. Renken, J. Catal. 219 (2003) 273–285.
[18] G.D. Pirngruber, M. Luechinger, P.K. Roy, A. Cecchetto, P. Smirniotis, J. Catal. 224 (2004) 429–440.
[19] G.D. Pirngruber, P.K. Roy, R. Prins, J. Catal. 246 (2007) 147–157.
[20] K. Sun, H. Xia, Z. Feng, R. van Santen, E. Hensen, C. Li, J. Catal. 254 (2008) 383–396.
[21] K. Jisa, J. Novakova, M. Schwarze, A. Vondrova, S. Sklenak, Z. Sobalik, J. Catal. 262 (2009) 27–34.
[22] H.Y. Chen, W.M.H. Sachtler, Catal. Lett. 50 (1998) 125–134.
[23] Q. Zhu, B.L. Mojet, R.A.J. Jansen, E.J.M. Hensen, J. van Grondelle, P.C.M.M. Magusin, R.A. van Santen, Catal. Lett. 81 (2002) 205–215.
[24] E.J.M. Hensen, Q. Zhu, M.M.R.M. Hendrix, A.R. Overveg, P.J. Kooyman, M.V. Sychev, R.A. van Santen, J. Catal. 221 (2004) 560–574.
[25] J.A.Z. Pieterse, S. Booneveld, R. van den Brink, Appl. Catal. B: Environ. 51 (2004) 215–228.
[26] J.-H. Park, J.-H. Choung, I.-S. Nam, S.-W. Ham, Appl. Catal. B: Environ. 78 (2008) 342–354.
[27] J. Perez-Ramirez, F. Kapteijn, J.C. Groen, A. Domenech, G. Mul, J.A. Moulijn, J. Catal. 214 (2003) 33–45.
[28] B.M. Abu-Zied, W. Schwieger, A. Unger, Appl. Catal. B: Environ. 84 (2008) 277–288.
[29] J. Perez-Ramirez, J. Catal. 227 (2004) 512–522.
[30] Ch. Song, B.H. Kim, C.R.F. Lund, J. Phys. Chem. B 109 (2005) 2295–2301.
[31] K. Sun, H. Xia, E. Hensen, R. van Santen, C. Li, J. Catal. 238 (2006) 186–195.
[32] P.K. Roy, R. Prins, G.D. Pirngruber, Appl. Catal. B: Environ. 80 (2008) 226–236.
[33] V.I. Sobolev, G.I. Panov, A.S. Kharitonov, V.N. Romannikov, A.M. Volodin, K.G. Ione, J. Catal. 139 (1993) 435–443.
[34] Q. Zhu, R.M. van Teeffelen, R.A. van Santen, E.J.M. Hensen, J. Catal. 221 (2004) 575–583.
[35] C.M. Fu, V.N. Korchak, W.K. Hall, J. Catal. 68 (1981) 166–171.
[36] F. Kapteijn, J. Rodriguez-Mirasol, J.A. Moulijn, J. Catal. 167 (1997) 256–265.
[37] B.R. Wood, J.A. Reimer, A.T. Bell, M.T. Janicke, K.C. Ott, J. Catal. 224 (2004) 148–155.
[38] E.M. El-Malki, R.A. van Santen, W.M.H. Sachtler, J. Catal. 196 (2000) 212–223.
[39] F.S. Stone, Adv. Catal. 13 (1962) 1.
[40] R.A. van Santen, M. Neurock, Molecular Heterogeneous Catalysis, WILEY–VCH, 2006.
[41] A.L. Yakovlev, G.M. Zhidomirov, R.A. van Santen, Catal. Lett. 75 (2001) 45–52.
[42] J.A. Ryder, A.K. Chakraborty, A.T. Bell, J. Catal. 220 (2003) 84–91.
[43] E.V. Kondratenko, J. Perez-Ramirez, J. Phys. Chem. B 110 (2006) 22586–22595.
[44] E.V. Kondratenko, V.A. Kondratenko, M. Santiago, J. Perez-Ramirez, J. Catal. 256 (2008) 248–258.
[45] T. Nobukawa, M. Yoshida, S. Kameoka, S. Ito, K. Tomishige, K. Kunimory, Stud. Surf. Sci. Catal. 154 (2004) 2514–2521.
[46] A. Guzman-Vargas, G. Delahay, B. Coq, Appl. Catal. B: Environ. 42 (2003) 369–379.
[47] M. Yoshida, T. Nobukawa, S. Ito, K. Tomishige, K. Kunimori, J. Catal. 223 (2004) 454–464.
[48] M.A.G. Hevia, J. Perez-Ramirez, Appl. Catal. B: Environ. 77 (2008) 248–254.
[49] Z. Sobalik, in: J. Cejka, J. Perez-Ramirez, W.J. Roth, Zeolites (Eds.), Transword Res. Netw. 37/661 (2) (2008) 1–24.
[50] A.A. Ivanov, V.S. Chernyavsky, M.J. Gross, A.S. Kharitonov, A.K. Uriarte, G.I. Panov, Appl. Catal. A: Gen. 249 (2003) 327–343.